INTERNATIONAL JOURNAL FOR NUMERICAL METHODS IN FLUIDS
Int. J. Numer. Meth. Fluids 2007; **54**:497–515
Published online 21 December 2006 in Wiley InterScience (www.interscience.wiley.com). DOI: 10.1002/fld.1407

Stability and approximability of the $\mathscr{P}_1$–$\mathscr{P}_0$ element for Stokes equations

Jinshui Qin[1] and Shangyou Zhang[2, *, †]

[1]*10321 Yellow Pine Dr., Vienna, VA 22182, U.S.A.*
[2]*Department of Mathematical Sciences, University of Delaware, DE 19716, U.S.A.*

SUMMARY

In this paper we study the stability and approximability of the $\mathscr{P}_1$–$\mathscr{P}_0$ element (continuous piecewise linear for the velocity and piecewise constant for the pressure on triangles) for Stokes equations. Although this element is unstable for all meshes, it provides optimal approximations for the velocity and the pressure in many cases. We establish a relation between the stabilities of the $\mathscr{Q}_1$–$\mathscr{P}_0$ element (bilinear/constant on quadrilaterals) and the $\mathscr{P}_1$–$\mathscr{P}_0$ element. We apply many stability results on the $\mathscr{Q}_1$–$\mathscr{P}_0$ element to the analysis of the $\mathscr{P}_1$–$\mathscr{P}_0$ element. We prove that the element has the optimal order of approximations for the velocity and the pressure on a variety of mesh families.

As a byproduct, we also obtain a basis of divergence-free piecewise linear functions on a mesh family on squares. Numerical tests are provided to support the theory and to show the efficiency of the newly discovered, truly divergence-free, $\mathscr{P}_1$ finite element spaces in computation. Copyright © 2006 John Wiley & Sons, Ltd.

Received 9 October 2005; Revised 16 October 2006; Accepted 17 October 2006

KEY WORDS: mixed finite elements; Stokes; divergence-free

1. INTRODUCTION

The $\mathscr{P}_1$–$\mathscr{P}_0$ element, continuous piecewise linear approximation for the velocity and piecewise constant approximation for the pressure, is probably the simplest finite element which could preserve the incompressibility condition of incompressible fluids (see [1–9] for more information on divergence-free elements for Stokes). Unfortunately, the element is unstable for any mesh since the dimension of the discrete velocity space is always less than that of the pressure space (with Dirichlet boundary condition). However, this element provides optimal approximations for both the velocity and the pressure on many mesh families. Some discussions on this element can be

*Correspondence to: Shangyou Zhang, Department of Mathematical Sciences, University of Delaware, DE 19716, U.S.A.
†E-mail: szhang@udel.edu

found in [4, 10–12] and references therein. In this paper, we concentrate on the triangular meshes made by crisscross-refinements of quadrilateral meshes, i.e. dividing each quadrilateral into four subtriangles by the two diagonals.

To make the notation in introduction clear, we define some notations first. Let $\mathbf{V}_h \subset \mathbf{H}^1(\Omega)$ and $P_h \subset L_0^2(\Omega) := L^2(\Omega)/C$ denote the mixed finite element spaces of velocity and pressure, respectively; they are defined on a triangulation $\mathscr{T}_h$ of a polygonal domain Ω. We solve the finite element approximation $(\mathbf{u}_h, p_h)$ satisfying the mixed formulation of Stokes equations

$$\begin{aligned} a(\mathbf{u}_h, \mathbf{v}) - b(\mathbf{v}, p_h) &= (\mathbf{f}, \mathbf{v}) \quad \forall \mathbf{v} \in \mathbf{V}_h \\ b(\mathbf{u}_h, q) &= 0 \quad \forall q \in P_h \end{aligned} \tag{1}$$

Here, $a(\mathbf{u}, \mathbf{v}) := \int_\Omega \nabla \mathbf{u} : \nabla \mathbf{v}$, $b(\mathbf{v}, q) := \int_\Omega q \operatorname{div} \mathbf{v}$, and $(\mathbf{f}, \mathbf{v}) := \int_\Omega \mathbf{f} \cdot \mathbf{v}$ for all $\mathbf{u}, \mathbf{v} \in \mathbf{V}_h$ and $q \in P_h$. For convenience, we define $N_h = \{q \in P_h | \int_\Omega q \operatorname{div} \mathbf{v} = 0, \forall \mathbf{v} \in \mathbf{V}_h\}$ and the reduced pressure space M_h as the L^2-orthogonal complement of N_h in P_h. The non-constant functions of N_h are called spurious pressure modes. The element $\mathbf{V}_h \times P_h$ is said to be stable if the inf–sup constant

$$\gamma_h(\mathbf{V}_h, P_h) := \inf_{0 \neq p \in P_h} \sup_{0 \neq \mathbf{v} \in \mathbf{V}_h} \frac{\int_\Omega p \operatorname{div} \mathbf{v}}{\|\mathbf{v}\|_{1,\Omega} \|p\|_{0,\Omega}}$$

is bounded below by a positive number independent of h, see [13, 14]. Here, P_h is assumed as a subset of L_0^2, i.e. $\int_\Omega q = 0$ for all $q \in P_h$. If $\mathbf{V}_h \times P_h$ is not stable but $\mathbf{V}_h \times M_h$ is, then the element $\mathbf{V}_h \times P_h$ is said to be reduced-stable. Accordingly, the inf–sup constant $\gamma_h(\mathbf{V}_h, M_h)$ is called the reduced inf–sup constant of the element $\mathbf{V}_h \times P_h$.

In this paper, we show a close relationship between the stabilities of the $\mathscr{Q}_1$–$\mathscr{P}_0$ element (bilinear/constant quadrilateral element) and the $\mathscr{P}_1$–$\mathscr{P}_0$ element. That is, the reduced stability of the $\mathscr{Q}_1$–$\mathscr{P}_0$ element on a family of quadrilateral meshes is equivalent to that for $\mathscr{P}_1$–$\mathscr{P}_0$ on the crisscross-refinement meshes of the quadrilateral family. Therefore, many results on the stability of the $\mathscr{Q}_1$–$\mathscr{P}_0$ element can be applied to $\mathscr{P}_1$–$\mathscr{P}_0$. For example, the reduced inf–sup constant of the $\mathscr{Q}_1$–$\mathscr{P}_0$ element is Ch on the square meshes of the unit square, therefore, the reduced inf–sup constant of the $\mathscr{P}_1$–$\mathscr{P}_0$ element on the crisscross meshes of the unit square is Ch too. There are many results on the stability and approximability of the $\mathscr{Q}_1$–$\mathscr{P}_0$ element (see [4, 5, 15–24].)

If a mesh family is stable for the $\mathscr{Q}_1$–$\mathscr{P}_0$ element, then the crisscross-refinement of the mesh family is reduced-stable for $\mathscr{P}_1$–$\mathscr{P}_0$. Then, we show that the $\mathscr{P}_1$–$\mathscr{P}_0$ element has optimal approximations for the velocity and pressure. There are a wide range of stable families for the quadrilateral element $\mathscr{Q}_1$–$\mathscr{P}_0$, see [25]. Therefore, the numerical solutions of the element $\mathscr{P}_1$–$\mathscr{P}_0$ are of the optimal order on the crisscross-refinements of all these families. The performance of the $\mathscr{P}_1$–$\mathscr{P}_0$ element on some general mesh families is also discussed in this paper.

As a byproduct of our analysis, we explicitly display a basis of all divergence-free continuous piecewise linear polynomials defined on the crisscross grids of the unit square (cf. Figure 1(a)). Each basis function has a small support formed by a few triangles. Moreover, we show that the space of these divergence-free functions has the optimal approximation property. The analysis is supported by a numerical test. We found that the only other study on divergence-free $\mathscr{P}_1$ elements is on the finite element with polar coordinates [26].

We need to point out that the C_0 divergence-free $\mathscr{P}_1$ vector space is the curl of C_1 $\mathscr{P}_2$ space on a same triangular grid. Therefore, from the two known C_1 $\mathscr{P}_2$ elements, the Powell–Sabin element and the Powell–Sabin–Heindl element, cf. [11, 27, 28], see also Figure 1(b)–(c), we can derive C_0

DOI: 10.1002/fld

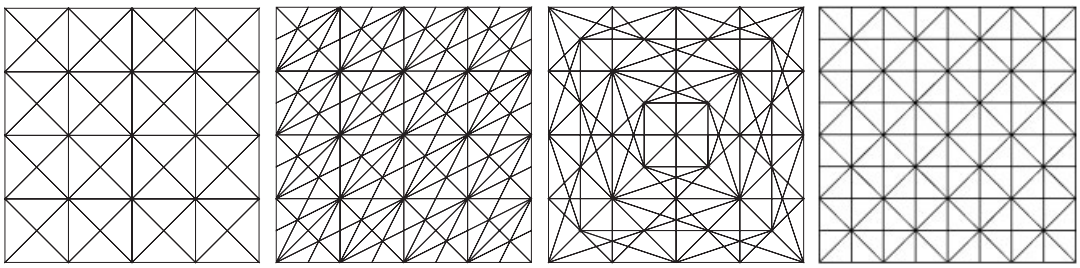

Figure 1. A crisscross, a Powell–Sabin, a Powell–Sabin–Heindl and a type-2 grid.

divergence-free $\mathscr{P}_1$ spaces too. It is obvious that the crisscross-type grids are much more efficient in computation than the Powell–Sabin and Clough–Tocher-type grids, cf. for example [29]. As we found a local basis for divergence-free $\mathscr{P}_1$ vector space, we can easily find their anti-derivatives to obtain a local basis for the C_1 $\mathscr{P}_2$ space on the crisscross grid. We note that such a local basis is not known previously. The method of representing a piecewise $C1$ polynomial basis without using nodal derivatives was reported previously in [30]. More work on such C_1 elements would be performed elsewhere. However, we comment that extensive studies have been done on a similar type of grids, the type-2 triangulation where the centre of each square is connected to both the four vertices and the four mid-edge points (see Figure 1(d)), cf. [31–33], and its counterpart in three-dimension, cf. [34–36].

There are six sections in the paper. In Section 2, we discuss the stability relation between $\mathscr{P}_1$–$\mathscr{P}_0$ and $\mathscr{Q}_1$–$\mathscr{P}_0$. In Section 3, we analyse the approximation properties of the $\mathscr{P}_1$–$\mathscr{P}_0$ element on the crisscross meshes of the unit square. We study the performance of the element on a general mesh family in Section 4. In Section 5, we display a basis of divergence-free piecewise linear functions. Finally in Section 6, we report some numerical results on the reduced stability and approximability of the $\mathscr{P}_1$–$\mathscr{P}_0$ element. We also illustrate the efficiency of using the newly discovered divergence-free basis in computation by a simple example.

2. STABILITIES OF $\mathscr{P}_1$–$\mathscr{P}_0$ AND $\mathscr{Q}_1$–$\mathscr{P}_0$ ELEMENTS

In this section, we shall study the relationship between $\mathscr{P}_1$–$\mathscr{P}_0$ and $\mathscr{Q}_1$–$\mathscr{P}_0$ finite elements. The Ω under consideration could be a general polygonal domain. We denote a quadrilateral partition of Ω by $\mathscr{Q}_h$ and its corresponding crisscross-refinement by $\mathscr{T}_h$, which is obtained by dividing each quadrilateral in $\mathscr{Q}_h$ by its two diagonals.

For each triangle $T \in \mathscr{T}_h$, let h_T denote the diameter of T and ρ_T the diameter of the circle inscribed in T. A family of triangulations of Ω is said to be regular if there is a positive θ independent of h such that

$$\frac{\rho_T}{h_T} \geqslant \theta \tag{2}$$

We assume triangulations are regular in this paper.

DOI: 10.1002/fld

Let $\hat{W}$ denote the unit square $[0, 1] \times [0, 1]$ with vertices $\hat{w}_1$, $\hat{w}_2$, $\hat{w}_3$, and $\hat{w}_4$ (counterclockwise from the left-lower corner). For any quadrilateral $W \in \mathscr{Q}_h$ with the vertices w_1, w_2, w_3, and w_4 (counterclockwise), there exists exactly one bilinear mapping $F_W \in \hat{Q}_1(\hat{W})^2$ that maps $\hat{W}$ onto W such that $F_W(\hat{w}_i) = w_i$. Here,

$$\hat{Q}_k(\hat{W}) = \left\{ \sum_{0 \leqslant i,j \leqslant k} a_{ij} \hat{x}^i \hat{y}^j | a_{ij} \in R \right\}$$

On the quadrilateral W, we define finite element space

$$Q_k(W) = \{v \circ F_W^{-1}, \forall v \in Q_k(\hat{W})\}$$

where $k \geqslant 1$. On $\mathscr{Q}_h$, we define

$$M_k^0(\mathscr{Q}_h) = \{v \in H^1(\Omega) | v|_W \in Q_k(W), \forall W \in \mathscr{Q}_h\}$$

$$M_k^{-1}(\mathscr{Q}_h) = \{v \in L^2(\Omega) | v|_W \in Q_k(W), \forall W \in \mathscr{Q}_h\}$$

The finite element $\mathscr{Q}_1$–$\mathscr{P}_0$ and its associated spaces are defined as

$$\begin{aligned} \tilde{\mathbf{V}}_h &= \mathbf{M}_1^0(\mathscr{Q}_h) \cap \mathbf{H}^1(\Omega) \\ \tilde{P}_h &= M_0^{-1}(\mathscr{Q}_h) \\ \tilde{N}_h &= \{q \in \tilde{P}_h | b(\mathbf{v}, q) = 0, \forall \mathbf{v} \in \tilde{\mathbf{V}}_h\} \\ \tilde{M}_h &= L^2\text{-orthogonal complement of } \tilde{N}_h \text{ in } \tilde{P}_h \end{aligned} \tag{3}$$

Let $P_k(T)$ denote the polynomials with degree less than or equal to k defined on each triangle $T \in \mathscr{T}_h$. On $\mathscr{T}_h$, we define

$$M_k^0(\mathscr{T}_h) = \{v \in H^1(\Omega) | v|_T \in P_k(T), \forall T \in \mathscr{T}_h\}$$

$$M_k^{-1}(\mathscr{T}_h) = \{v \in L^2(\Omega) | v|_T \in P_k(T), \forall T \in \mathscr{T}_h\}$$

For the $\mathscr{P}_1$–$\mathscr{P}_0$ element, we use the notations $\mathbf{V}_h$, P_h, N_h, M_h, as defined by

$$\begin{aligned} \mathbf{V}_h &= \mathbf{M}_1^0(\mathscr{T}_h) \cap \mathbf{H}^1(\Omega) \\ P_h &= M_0^{-1}(\mathscr{T}_h) \\ N_h &= \{q \in P_h | b(\mathbf{v}, q) = 0, \forall \mathbf{v} \in \mathbf{V}_h\} \\ M_h &= L^2\text{-orthogonal complement of } N_h \text{ in } P_h \end{aligned} \tag{4}$$

It is obvious that $\tilde{P}_h \subset P_h$.

We call a polygonal region U of $\mathscr{T}_h$ (resp. $\mathscr{Q}_h$) a macroelement if it is formed by some triangles of $\mathscr{T}_h$ (resp. quadrilaterals of $\mathscr{Q}_h$). For a macroelement U of $\mathscr{T}_h$ (resp. $\mathscr{Q}_h$), we define localizations

DOI: 10.1002/fld

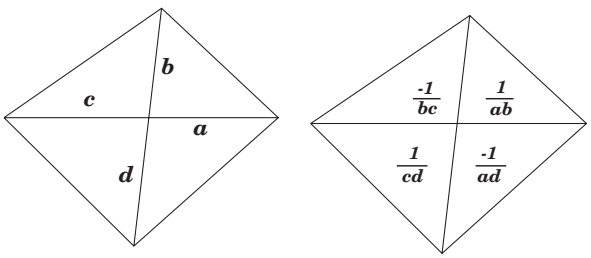

Figure 2. Macroelement U and spurious pressure mode δ_U.

$\mathbf{V}_h^U$, P_h^U, N_h^U, and M_h^U (resp. $\tilde{\mathbf{V}}_h^U$, $\tilde{P}_h^U$, $\tilde{N}_h^U$, and $\tilde{M}_h^U$) to U of the finite element spaces $\mathbf{V}_h$, P_h, N_h, and M_h (resp. $\tilde{\mathbf{V}}_h$, $\tilde{P}_h$, $\tilde{N}_h$, and $\tilde{M}_h$) by just replacing Ω by U in (3) (resp. (4)).

Lemma 2.1
Let $\mathscr{Q}_h$ be a quadrilateral partition of a polygonal domain Ω. If $\mathscr{T}_h$ is the corresponding crisscross-refinement for $\mathscr{Q}_h$, then

$$\tilde{N}_h \subset N_h$$

Proof
We note a simple fact first. For any $\mathbf{v} \in \mathbf{V}_h$, there exists a $\mathbf{w} \in \tilde{\mathbf{V}}_h$ such that

$$b(\mathbf{v}, q) = b(\mathbf{w}, q) \quad \forall q \in \tilde{P}_h \tag{5}$$

Similarly, for any $\mathbf{w} \in \tilde{\mathbf{V}}_h$, there is $\mathbf{v} \in \mathbf{V}_h$ such that (5) holds.

Since any function $\mathbf{w} \in \tilde{\mathbf{V}}_h$ is linear on all the edges of $\mathscr{Q}_h$, there exists a function $\mathbf{v} \in \mathbf{V}_h$ such that $\mathbf{v} - \mathbf{w}$ vanishes on all the edges of $\mathscr{Q}_h$. Therefore, (5) follows by using the Green's formula.

From (5), the lemma follows. □

In order to study the structure of N_h, we consider $\mathscr{Q}_h$ as a macroelement partition of $\mathscr{T}_h$. For any quadrilateral $U \in \mathscr{Q}_h$, there is a one-dimensional space of spurious pressure modes, with their support in U, associated with the singular vertex of U (the intersection of the two diagonals of U, see Figure 2). For convenience, we denote the spurious pressure mode, shown in the second picture of Figure 2, by δ_U (values of δ_U are shown in Figure 2, where a, b, c, and d are the lengths of the four interior edges). A detailed calculation of δ_U can be found in [7].

Lemma 2.2
Let $\mathscr{T}_h$ be the crisscross-refinement of $\mathscr{Q}_h$, then

$$N_h = \tilde{N}_h + \text{span}\{\delta_U | \text{ for all quadrilaterals } U \in \mathscr{Q}_h\}$$

Proof
Clearly, $\delta_U \in N_h$ for any $U \in \mathscr{Q}_h$. Since N_h^U contains only linear combinations of χ^U (the characteristic function of U) and δ_U for each $U \in \mathscr{Q}_h$, any function $q \in N_h$ must be in $\tilde{P}_h$ provided q is orthogonal to all δ_U's. By (5), $q \in \tilde{N}_h$. Hence, the lemma follows. □

DOI: 10.1002/fld

Corollary 2.1

$$M_h \cap \tilde{P}_h = \tilde{M}_h$$

Theorem 2.1
For a polygonal domain Ω, let $\mathscr{Q}_h$ be a quadrilateral partition of Ω and $\mathscr{T}_h$ be the corresponding crisscross-refinement. Assume $\mathscr{T}_h$ is regular. Then,

$$C\gamma_h(\tilde{\mathbf{V}}_h, \tilde{M}_h) \leqslant \gamma_h(\mathbf{V}_h, M_h) \leqslant C^{-1}\gamma_h(\tilde{\mathbf{V}}_h, \tilde{M}_h)$$

where C is independent of h.

Proof
Let $\mathscr{Q}_h$ be a macroelement partition of $\mathscr{T}_h$. On each macroelement $U \in \mathscr{Q}_h$, we have

$$\dim \mathbf{V}_h^U = 2, \quad \dim P_h^U = 4$$

$$\dim M_h^U = 2, \quad \dim N_h^U = 2$$

Following the arguments of Theorem 4.3.1 in [7], we can bound the local inf–sup constants $\gamma_h(\mathbf{V}_h^U, M_h^U)$ on all macroelements U in $\mathscr{Q}_h$ by a positive number which is independent of h. Applying the macroelement partition theorem (Theorem 3.2.1 in [7]), we know that the reduced inf–sup constant $\gamma_h(\mathbf{V}_h, M_h)$ is determined by the stability of $\mathbf{V}_h \times (M_h \cap \sum_{U \in \mathscr{Q}_h} N_h^U) = \mathbf{V}_h \times \tilde{M}_h$ (by the corollary). This implies that $\mathbf{V}_h \times M_h$ has exactly the same stability as $\mathbf{V}_h \times \tilde{M}_h$. If it is shown that $\mathbf{V}_h \times \tilde{M}_h$ and $\tilde{\mathbf{V}}_h \times \tilde{M}_h$ have the same stability, then the theorem is proven.

We first show that

$$\gamma_h(\mathbf{V}_h, M_h) \leqslant C^{-1}\gamma_h(\tilde{\mathbf{V}}_h, \tilde{M}_h) \tag{6}$$

For any $q \in \tilde{M}_h$, there exists a function $\mathbf{w} \in \tilde{\mathbf{V}}_h$ such that

$$\begin{aligned} b(\mathbf{w}, q) &= \|q\|_{0,\Omega}^2 \\ \|\mathbf{w}\|_{1,\Omega} &\leqslant \frac{C}{\gamma_h(\tilde{\mathbf{V}}_h, \tilde{M}_h)}\|q\|_{0,\Omega} \end{aligned} \tag{7}$$

If we can construct a function $\mathbf{v} \in \mathbf{V}_h$ such that

$$b(\mathbf{v}, q) = \|q\|_{0,\Omega}^2$$

$$\|\mathbf{v}\|_{1,\Omega} \leqslant \frac{C}{\gamma_h(\tilde{\mathbf{V}}_h, \tilde{M}_h)}\|q\|_{0,\Omega}$$

then (6) is proved.

Let $\mathbf{I}_h := (I_h, I_h)\colon \tilde{\mathbf{V}}_h \to \mathbf{V}_h$ be the interpolation operator such that $\mathbf{I}_h\mathbf{g}$ and $\mathbf{g}$ agree at every vertex in $\mathscr{T}_h$ for any $\mathbf{g} \in \tilde{\mathbf{V}}_h$. For any function $\mathbf{g} \in \tilde{\mathbf{V}}_h$, the interpolation error $\mathbf{g} - \mathbf{I}_h\mathbf{g}$ vanishes at all the edges of the quadrilateral partition $\mathscr{Q}_h$. We will show that there is a constant C independent

DOI: 10.1002/fld

of h such that

$$\|\mathbf{g} - \mathbf{I}_h\mathbf{g}\|_{1,\Omega} \leqslant C\|\mathbf{g}\|_{1,\Omega} \tag{8}$$

for any $\mathbf{g} \in \tilde{\mathbf{V}}_h$. If this is the case, by taking $\mathbf{v} = \mathbf{I}_h\mathbf{w}$, then

$$\|\mathbf{v}\|_{1,\Omega} \leqslant \|\mathbf{w} - \mathbf{v}\|_{1,\Omega} + \|\mathbf{w}\|_{1,\Omega} \leqslant C\|\mathbf{w}\|_{1,\Omega}$$

According to the arguments in the proof of Lemma 2.1 and (7), we have

$$b(\mathbf{v}, q) = b(\mathbf{w}, q) = \|q\|_{0,\Omega}^2$$

$$\|\mathbf{v}\|_{1,\Omega} \leqslant \frac{C}{\gamma_h(\tilde{\mathbf{V}}_h, \tilde{M}_h)}\|q\|_{0,\Omega}$$

This proves (6) with assumption (8).

Let $U \in \mathscr{Q}_h$ be a macroelement. If we need to show that

$$\|g - I_h g\|_{0,U} \leqslant C\|g\|_{0,U} \tag{9}$$

$$|g - I_h g|_{1,U} \leqslant C|g|_{1,U} \tag{10}$$

for any $g \in Q_1(U)$, any $U \in \mathscr{Q}_h$, and any $h>0$ with constant C independent of h. Let $E_\theta(\hat{U})$ denote the set of all the equivalence macroelements, see [1, 7, 25], of the unit square $\hat{U}$ satisfying the regularity condition (2). Obviously, translations and dilations of U do not affect (9) and (10). Therefore, for simplicity, we assume that the length of the longest diagonals of each macroelement in $E_\theta(\hat{U})$ is one unit, and that the intersection of the two diagonals of any macroelement in $E_\theta(\hat{U})$ has coordinates $(0, 0)$. For any macroelement U in $E_\theta(\hat{U})$, we denote the intersection of its two diagonals by v_5 and the other four vertices by v_1, v_2, v_3, and v_4, clockwise. Hence, $S = \{(v_1, v_2, v_3, v_4, v_5) \mid U \in E_\theta(\hat{U})\}$ is a closed set in $\mathbf{R}^{10}$. Let $g \in Q_1(U)$ be arbitrary and its value at v_i be g_i for $i = 1, 2, 3, 4$. For convenience, we denote the vector $(g_1, g_2, g_3, g_4)^{\mathrm{t}}$ by $\bar{g}$. Since $(I_h g)(v_i) = g_i$ for $i = 1, 2, 3, 4$ and $(I_h g)(v_5)$ is determined by g_1, g_2, g_3, and g_4, we have

$$\|g - I_h g\|_{0,U}^2 = \bar{g}^{\mathrm{t}} A_U \bar{g}$$

$$\|g\|_{0,U}^2 = \bar{g}^{\mathrm{t}} B_U \bar{g}$$

$$|g - I_h g|_{1,U}^2 = \bar{g}^{\mathrm{t}} C_U \bar{g}$$

$$|g|_{1,U}^2 = \bar{g}^{\mathrm{t}} D_U \bar{g}$$

Here, B_U is a symmetric positive definite and A_U, C_U, and D_U are symmetric positive semi-definite. Clearly, the entries of A_U, B_U, C_U, and D_U are continuous functions of $(v_1, \ldots, v_5)$.

Since S is a bounded closed set in $\mathbf{R}^{10}$, there exists a constant C_1 independent of h such that

$$\|g - I_h g\|_{0,U} \leqslant C_1\|g\|_{0,U} \tag{11}$$

for any $U \in E_\theta(\hat{U})$.

DOI: 10.1002/fld

It is easy to see that only the constant functions make both sides of (10) zero. Hence, the matrix D_U always has exactly three positive eigenvalues which depend on $(v_1, v_2, v_3, v_4, v_5)$ continuously. Since S is a bounded closed set in $\mathbf{R}^{10}$, the smallest non-zero eigenvalue of D_U is bounded away from zero by a positive number independent of h. Due to the same reason, the largest eigenvalue of C_U is bounded above by a constant independent of h. Therefore, there exists a constant C_2 independent of h such that

$$|g - I_h g|_{1,U} \leqslant C_2 |g|_{1,U} \tag{12}$$

for any $U \in E_\theta(\hat{U})$.

Combining (11) and (12), we obtain (9) and (10). Therefore, we have proven (6). Using similar arguments, we can show that $\tilde{\gamma}_h \geqslant C\bar{\gamma}_h$. □

Theorem 2.2

Let $\mathscr{Q}_h$ be a quadrilateral partition of a polygonal domain Ω and $\mathscr{T}_h$ be the corresponding crisscross-refinement. If $\tilde{\mathbf{V}}_h \times \tilde{P}_h$ is stable, then $\mathbf{V}_h \times M_h$ is stable. Moreover, if $(\mathbf{u}_h, \bar{p}_h) \in \mathbf{V}_h \times M_h$ and $(\mathbf{u}_h, p_h) \in \mathbf{V}_h \times P_h$ solve (1), then

$$\begin{aligned} \|\mathbf{u} - \mathbf{u}_h\|_{1,\Omega} &\leqslant Ch\|\mathbf{u}\|_{2,\Omega} \\ \|p - \bar{p}_h\|_{0,\Omega} &\leqslant Ch(\|\mathbf{u}\|_{2,\Omega} + \|p\|_{1,\Omega}) \end{aligned} \tag{13}$$

Here, the constant C is independent of h, $\bar{p}_h = p_h / N_h$, and we assume that $(\mathbf{u}, p) \in \mathring{\mathbf{H}}^2(\Omega) \times H^1(\Omega)$ solves the Stokes equations on the continuous level.

Proof

Stability of $\mathbf{V}_h \times M_h$ is a direct consequence of Theorem 2.1. It is known that $M_0^{-1}(\mathscr{Q}_h)/\mathbf{R} \subset M_h$ implies that the approximation properties of M_h are as good as those of P_h. Therefore, by the stability theorem established in [14], (13) follows (the error estimate of velocity is decoupled from $\|p\|_{1,\Omega}$ because of $\operatorname{div} \mathbf{u}_h = 0$). □

For the $\mathscr{Q}_1$–$\mathscr{P}_0$ element, one stable mesh family was identified in [25]. On the crisscross-refinements of all these stable families, the $\mathscr{P}_1$–$\mathscr{P}_0$ element is reduced-stable and the numerical solution is optimal.

The pressure $\bar{p}_h \in M_h$ can be recovered from $p_h \in P_h$ by applying a simple postprocess quadrilateral by quadrilateral. That is, on each quadrilateral $U \in \mathscr{Q}_h$,

$$\bar{p}_h|_U = p_h|_U - \frac{\int_U p_h \delta_U}{\int_U \delta_U^2} \delta_U$$

As a direct application of Lemma 2.2, Theorem 2.1, and the stability results of the element $\mathscr{Q}_1$–$\mathscr{P}_0$ in [5, 15, 25], we get the following theorem.

Theorem 2.3

Let $\mathscr{Q}_h$, $h = 1/n$, be a square mesh of the unit square and $\mathscr{T}_h$ be the corresponding crisscross-refinement. Then

$$\gamma_h(\mathbf{V}_h, M_h) = Ch, \quad \dim N_h = n^2 + 2$$

However, the approximation properties of the numerical solution of the $\mathscr{P}_1$–$\mathscr{P}_0$ element on the crisscross-refinement (the mesh is also called crisscross mesh) of the square mesh of the unit

DOI: 10.1002/fld

square cannot be answered directly by applying the stability theorem established in [14] since the reduced inf–sup constant is Ch. This will be answered in the next section.

3. APPROXIMATION PROPERTIES ON CRISSCROSS MESHES

In this section, we show that the numerical solutions of (1) converge to the true solution of the Stokes equations (with Dirichlet boundary condition) at a rate of h on the crisscross meshes of the unit square. Moreover, we will display a way to recover the numerical solution for the pressure. Since $\mathbf{V}_h \times M_h$ is unstable, this means that M_h is still too large. Therefore, we need to remove more modes from M_h while trying to preserve the approximation properties for the remaining pressure space S_h. It is then necessary to define a new velocity space $\mathbf{W}_h \subset \mathbf{V}_h$ such that not only is $\mathbf{W}_h \times S_h$ stable but also the velocity from $\mathbf{W}_h \times S_h$ is exactly the same as $\mathbf{u}_h$ from $\mathbf{V}_h \times M_h$. Of course, the space $\mathbf{W}_h$ should possess good approximation properties.

The crucial matter here is to determine the bad modes in M_h. Let $h = 1/n$ and $n = 4k$ for some positive integer k, and let $\mathscr{T}_h$ be the crisscross mesh of the unit square. For convenience, we denote (α, β) the vertex in $\mathscr{T}_h$ with coordinates $(\alpha h, \beta h)$, and $\delta_{\alpha+1/2,\beta+1/2}$ the spurious pressure mode associated with the singular vertex (α, β) (see Figure 3). Let $\mathscr{Q}_{4h}$ be a macroelement partition of $\mathscr{T}_h$ such that every $U \in \mathscr{Q}_{4h}$ has 16 $h \times h$ squares. Therefore, U consists of 64 triangles. From Lemma 2.2, we know that N_h^U is the space spanned by the functions χ^U (the characteristic function with support U), δ_U (the checkerboard mode with support U, shown in Figure 3), and $\delta_{i+1/2,j+1/2}$, where $(i+1/2,\ j+1/2)$ is a singular vertex in U. Obviously, the $\delta_{i+1/2,j+1/2}$'s are not in M_h. Since the global checkerboard mode $\delta_\Omega \in \text{span}\{\delta_U, \forall U \in \mathscr{Q}_{4h}\}$, we need to remove $\text{span}\{\delta_U, \forall U \in \mathscr{Q}_{4h}\}$ from M_h.

Define

$$\bar{N}_h = \text{span}\{1,\ \delta_{i+1/2,j+1/2},\ \delta_U,\ 1 \leqslant i,\ j \leqslant n-1,\ \forall U \in \mathscr{Q}_{4h}\}$$

$$S_h = L^2\text{-orthogonal complement of } \bar{N}_h \text{ in } P_h$$

$$\mathbf{W}_h = \{\mathbf{v} \in \mathbf{V}_h | b(\mathbf{v}, q) = 0,\ \forall q \in \bar{N}_h\}$$

$$S_h^U = \chi^U S_h$$

$$\mathbf{W}_h^U = \{\mathbf{v} \in \mathbf{W}_h | \text{support } \mathbf{v} \subset U\}$$

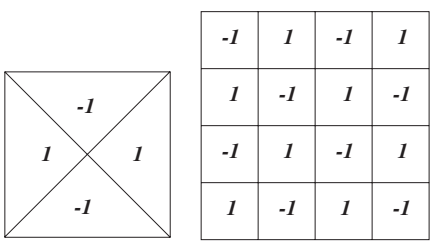

Figure 3. $\delta_{\alpha+1/2,\beta+1/2}$ and δ_U.

DOI: 10.1002/fld

Theorem 3.1
Let $\mathscr{T}_h$ be a crisscross mesh of the unit square. Assume $(\mathbf{u}, p) \in \mathring{\mathbf{H}}^2(\Omega) \times H^1(\Omega)$ is the true solution of the Stokes equations and $(\tilde{\mathbf{u}}_h, \tilde{p}_h) \in \mathbf{W}_h \times S_h$ solves (1), then

$$\|\mathbf{u} - \tilde{\mathbf{u}}_h\|_{1,\Omega} \leqslant Ch\|\mathbf{u}\|_{2,\Omega}$$

$$\|p - \tilde{p}_h\|_{0,\Omega} \leqslant Ch(\|\mathbf{u}\|_{2,\Omega} + \|p\|_{1,\Omega})$$

Proof
It is easy to verify that

$$N_h \subset \bar{N}_h, \quad \mathbf{M}_1^0(\mathscr{T}_{2h}) \cap \mathring{\mathbf{H}}^1(\Omega) \subset \mathbf{W}_h \quad \text{and} \quad M_0^{-1}(\mathscr{Q}_{4h}) \subset S_h$$

Therefore, $\mathbf{W}_h \times S_h$ has good approximation properties. It only remains to prove that $\mathbf{W}_h \times S_h$ is stable.

Define

$$\tilde{N}_h^U = \{q \in S_h^U \,|\, b(\mathbf{v}, q) = 0, \forall \mathbf{v} \in \mathbf{W}_h^U\}$$

Then, Lemma 2.2 implies that $\tilde{N}_h^U$ contains only constant functions. Therefore, $\mathbf{W}_h \times (S_h \cap (\bigcup_{U \in \mathscr{Q}_{4h}} \tilde{N}_h^U))$ is stable by the fact that $[\mathbf{M}_1^0(\mathscr{T}_{2h}) \cap \mathring{\mathbf{H}}^1(\Omega)] \times M_0^{-1}(\mathscr{Q}_{4h})$ is stable. Finally, by using the macroelement partition theorem, see [1, 7, 25], we have that $\mathbf{W}_h \times S_h$ is stable. □

Theorem 3.2
Let $\mathscr{T}_h$ be the crisscross mesh of the unit square with $h = 1/(4k)$ for some positive integer k. If $(\mathbf{u}, p) \in \mathring{\mathbf{H}}^2(\Omega) \times H^1(\Omega)$ is the true solution of the Stokes equations, then the solution $(\mathbf{u}_h, p_h) \in \mathbf{V}_h \times P_h$ of (1) satisfies

$$\|\mathbf{u} - \mathbf{u}_h\|_{1,\Omega} \leqslant Ch\|\mathbf{u}\|_{2,\Omega}$$

$$p_h = \tilde{p}_h + \bar{N}_h$$

and the pressure can be recovered from p_h by a postprocess.

Proof
Clearly, the solution $(\mathbf{u}_h, p_h) \in \mathbf{V}_h \times P_h$ of

$$a(\mathbf{u}_h, \mathbf{v}) + b(\mathbf{v}, p_h) = (\mathbf{f}, \mathbf{v}) \quad \forall \mathbf{v} \in \mathbf{V}_h$$

$$b(\mathbf{u}_h, q) = 0 \quad \forall q \in P_h$$

satisfies

$$\begin{aligned} a(\mathbf{u}_h, \mathbf{v}) + b(\mathbf{v}, p_h) &= (\mathbf{f}, \mathbf{v}) \quad \forall \mathbf{v} \in \mathbf{W}_h \\ b(\mathbf{u}_h, q) &= 0 \quad \forall q \in S_h \end{aligned} \tag{14}$$

DOI: 10.1002/fld

Since $\mathbf{u}_h \in \mathbf{W}_h$ and $p_h = (p_h/\bar{N}_h) + n_h$ for some $n_h \in \bar{N}_h$, (14) implies

$$a(\mathbf{u}_h, \mathbf{v}) + b(\mathbf{v}, p_h/\bar{N}_h) = (\mathbf{f}, \mathbf{v}) \quad \forall \mathbf{v} \in \mathbf{W}_h$$

$$b(\mathbf{u}_h, q) = 0 \quad \forall q \in S_h$$

Since the solution of (1) in $\mathbf{W}_h \times S_h$ is unique, we get

$$\mathbf{u}_h = \tilde{\mathbf{u}}_h \quad \text{and} \quad p_h/\bar{N}_h = \tilde{p}_h$$

By Theorem 3.1, the velocity $\mathbf{u}_h$ and recovered pressure $\tilde{p}_h$ have optimal rates of convergence. It is simple to recover $\tilde{p}_h$ from p_h since $\bar{N}_h$ is known. □

4. APPROXIMATION PROPERTIES ON A GENERAL MESH FAMILY

The $\mathscr{P}^1$–$\mathscr{P}^0$ element is further analysed on a general mesh family in this section. On this family of meshes, it is shown that the finite element solution for the velocity converges at an order h and the pressure can be recovered by a simple postprocess.

The triangulation $\mathscr{T}_h$ is formed in the following way. First, we partition the polygonal domain Ω into quadrilaterals. This quadrilateral partition is denoted by $\mathscr{Q}_{4h}$. Secondly, each quadrilateral in $\mathscr{Q}_{4h}$ is divided into four sub-quadrilaterals by linking the intersection of its two diagonals to the middle point of each edge, so $\mathscr{Q}_{2h}$ is formed. Repeating the above process to all quadrilaterals in $\mathscr{Q}_{2h}$, we have $\mathscr{Q}_h$. Finally, partitioning each quadrilateral in $\mathscr{Q}_h$ into four triangles by its two diagonals, we obtain the triangulation $\mathscr{T}_h$. The first figure in Figure 4 shows how to partition a quadrilateral in $\mathscr{Q}_{4h}$ into four quadrilaterals in $\mathscr{Q}_{2h}$. The second figure shows a macroelement in $\mathscr{Q}_{4h}$ with 64 triangles in $\mathscr{T}_h$.

We will show that on the triangulation $\mathscr{T}_h$, the numerical solution $\mathbf{u}_h$ has an optimal rate of convergence and a pressure with an optimal rate of convergence can be recovered from p_h. The measure to achieve this objective is quite similar to what we used for the crisscross mesh. We first remove all possible 'bad modes' from P_h, and then consider the pressure in the remaining pressure space. The key issue is to determine bad pressure modes in P_h. We know that spurious pressure modes associated with each singular vertex must be removed from the pressure space P_h. However, this is not enough to guarantee the stability according to our experience with the crisscross mesh. Since the crisscross mesh is a special case of $\mathscr{T}_h$, we definitely need to remove those pressure modes which may degenerate to local spurious modes. Based on this consideration,

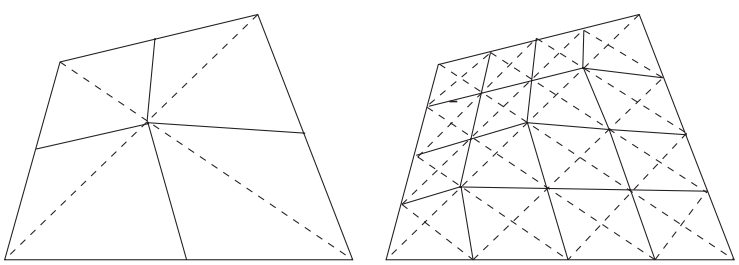

Figure 4. Form $\mathscr{Q}_h$ from $\mathscr{Q}_{4h}$.

DOI: 10.1002/fld

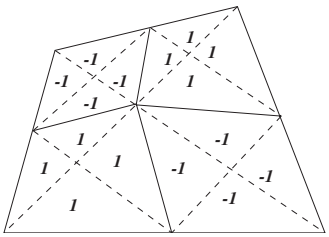

Figure 5. 'Bad pressure mode' over U_{2h}.

we will remove all multiples of the mode (shown in Figure 5) on each macroelement in $\mathscr{Q}_{2h}$ from the pressure space P_h.

For convenience, we denote a quadrilateral in $\mathscr{Q}_h$ by U_h, a quadrilateral in $\mathscr{Q}_{2h}$ by U_{2h}, and a quadrilateral in $\mathscr{Q}_{4h}$ by U_{4h}. We also denote the mode shown in Figure 5 by $\delta_{U_{2h}}$. Let δ_{U_h} denote the spurious pressure mode associated with the singular vertex in $U_h \in \mathscr{Q}_h$. We can easily conclude that

$$\int_T \delta_{U_{2h}} = 0$$

for any $T \in \mathscr{T}_{2h}$, any $U_{2h} \in \mathscr{Q}_{2h}$.

Define

$$\bar{N}_h = \text{span}\{1, \delta_{U_h}, \delta_{U_{2h}}, \forall U_h \in \mathscr{Q}_h, \forall U_{2h} \in \mathscr{Q}_{2h}\}$$

$$S_h = L^2\text{-orthogonal complement of } \bar{N}_h \text{ in } P_h$$

$$\mathbf{W}_h = \{\mathbf{v} \in \mathbf{V}_h | b(\mathbf{v}, q) = 0, \forall q \in \bar{N}_h\}$$

$$S_h^{U_{4h}} = \chi^{U_{4h}} S_h$$

$$\mathbf{W}_h^{U_{4h}} = \{\mathbf{v} \in \mathbf{W}_h | \text{support } \mathbf{v} \subset U_{4h}\}$$

Theorem 4.1

Let $\mathscr{T}_h$ be a regular triangulation defined above. If $(\mathbf{u}, p) \in \mathring{\mathbf{H}}^2(\Omega) \times H^1(\Omega)$ is the true solution of the Stokes equations and $(\tilde{\mathbf{u}}_h, \tilde{p}_h) \in \mathbf{W}_h \times S_h$ solves (1), then

$$\|\mathbf{u} - \tilde{\mathbf{u}}_h\|_{1,\Omega} \leqslant Ch\|\mathbf{u}\|_{2,\Omega}$$

$$\|p - \tilde{p}_h\|_{0,\Omega} \leqslant Ch(\|\mathbf{u}\|_{2,\Omega} + \|p\|_{1,\Omega})$$

Proof

It is expected that $N_h \subset \bar{N}_h$, if $\mathscr{T}_h$ is a crisscross mesh. Since $\mathscr{T}_h^{U_{4h}}$ has the special structure, we can show that

$$M_0^{-1}(\mathscr{Q}_{4h}) \subset S_h \quad \text{and} \quad [\mathbf{M}_1^0(\mathscr{T}_{2h}) \cap \mathring{\mathbf{H}}^1(\Omega)] \subset \mathbf{W}_h$$

DOI: 10.1002/fld

Therefore, $\mathbf{W}_h \times S_h$ has good approximation properties. If we can prove that $\mathbf{W}_h \times S_h$ is stable, then the proof is done.

Define

$$\tilde{N}_h^{U_{4h}} = \{q \in S_h^{U_{4h}} | b(\mathbf{v}, q) = 0, \forall \mathbf{v} \in \mathbf{W}_h^{U_{4h}}\}$$

We need to show that $\tilde{N}_h^{U_{4h}}$ contains only constant functions. If it does for any $U_{4h} \in \mathscr{Q}_{4h}$, then $\mathbf{W}_h \times (S_h \cap (\cup_{U_{4h} \in \mathscr{Q}_{4h}} \tilde{N}_h^{U_{4h}}))$ is stable by the fact that $[\mathbf{M}_1^0(\mathscr{T}_{2h}) \cap \mathring{\mathbf{H}}^1(\Omega)] \times M_0^{-1}(\mathscr{Q}_{4h})$ is stable. Therefore, by using the macroelement partition theorem we can prove that $\mathbf{W}_h \times S_h$ is stable.

We show that $\dim \tilde{N}_h^{U_{4h}} = 1$. Since $\delta_{U_h} \in \bar{N}_h$, if $q \in \tilde{N}_h^{U_{4h}}$, then q is a constant on each U_h in U_{4h}. Hence, q must be a constant on each U_{2h} in U_{4h} since we already removed $\delta_{U_{2h}}$ from the pressure space. Therefore, q must be a constant on each of the four U_{2h} in U_{4h}. A simple computation shows that q must be a constant on U_{4h}. □

Theorem 4.2

Let $\mathscr{T}_h$ be the triangulation defined at the beginning of this section, from a specially constructed $\mathscr{Q}_h$, then the numerical solution $(\mathbf{u}_h, p_h) \in \mathbf{V}_h \times P_h$ satisfies

$$\|\mathbf{u} - \mathbf{u}_h\|_{1,\Omega} \leqslant Ch\|\mathbf{u}\|_{2,\Omega}$$

and $p_h / \bar{N}_h = \tilde{p}_h$. Here, we assume $(\mathbf{u}, p) \in \mathring{\mathbf{H}}^2(\Omega) \times H^1(\Omega)$ solves the Stokes equations.

Proof

Use similar arguments as in the proof of Theorem 3.2. □

5. A BASIS OF DIVERGENCE-FREE PIECEWISE LINEAR FUNCTIONS

In this section, we display a basis for $\mathbf{Z}_h$, the space of all divergence-free continuous piecewise linear polynomials on the crisscross mesh $\mathscr{T}_h$. All the basis functions have a very small local support and the space $\mathbf{Z}_h$ has optimal approximation properties.

Let the domain Ω be the unit square and $\mathscr{Q}_h$, $h = 1/n$ a partition of Ω which contains $n \times n$ equal small squares. The triangulation $\mathscr{T}_h$ is the crisscross-refinement of $\mathscr{Q}_h$.

Define

$$\mathbf{V}_h = \mathbf{M}_1^0(\mathscr{T}_h) \cap \mathring{\mathbf{H}}^1(\Omega)$$

$$\mathbf{Z}_h = \{\mathbf{v} \in \mathbf{V}_h | \operatorname{div} \mathbf{v} = 0\}$$

A simple calculation shows that

$$\dim \mathbf{V}_h = 4n^2 - 4n + 2$$

In order to study $\mathbf{Z}_h$, we define a 'pressure' space P_h as

$$P_h = M_0^{-1}(\mathscr{T}_h)$$

The analysis of the properties of $\mathbf{Z}_h$ can be carried out using the frame work of the analysis of the $\mathscr{P}_1$–$\mathscr{P}_0$ finite element for the Stokes equations with Dirichlet boundary conditions.

DOI: 10.1002/fld

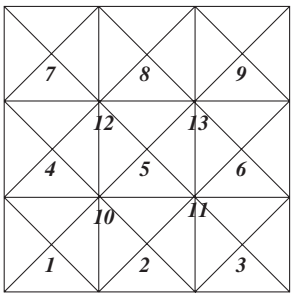

Figure 6. Macroelement U.

Since $\operatorname{div} \mathbf{V}_h \subset P_h$, we have

$$\mathbf{Z}_h = \{\mathbf{v} \in \mathbf{V}_h | \operatorname{div} \mathbf{v} = 0\} = \{\mathbf{v} \in \mathbf{V}_h | b(\mathbf{v}, q) = 0, \forall q \in P_h\}$$

Lemma 5.1
On the crisscross triangulation $\mathscr{T}_h$ with $h = 1/n$,

$$\dim \mathbf{Z}_h = (n-2)^2$$

Proof
Since $\dim P_h = 4n^2$ and $\dim N_h = n^2 + 2$ (see Theorem 2.3), the lemma holds. □

In order to find a basis for $\mathbf{Z}_h$, we first consider a small macroelement U with size $3h \times 3h$ (see Figure 6).

We denote the interior vertices of U by $1, 2, \ldots, 13$, as shown in Figure 6, and denote the nodal basis functions by $\phi_1, \phi_2, \ldots, \phi_{13}$ accordingly. Let $\mathbf{V}_h^U$ denote the subspace of $\mathbf{V}_h$ such that all the functions in $\mathbf{V}_h^U$ have supports contained in U. We look for functions $\mathbf{v} = \sum_{i=1}^{13} (u_i, v_i)\phi_i \in \mathbf{V}_h^U$ such that $\operatorname{div} \mathbf{v} = 0$ in U. Namely, we need to solve a system of 36 linear equations in 26 unknowns. Since $\dim \mathbf{Z}_h^U = 1$, we know that this system has a one-dimensional solution space. After some algebraic computations, we find that the solution space is

$$\mathbf{Z}_h^U = \operatorname{span}\{\mathbf{z}^U\}$$

where $\mathbf{z}^U = (\xi, \eta)$ and

$$\xi = \phi_2 - \phi_8 + \phi_{10} + \phi_{11} - \phi_{12} - \phi_{13}$$

$$\eta = -\phi_4 + \phi_6 - \phi_{10} + \phi_{11} - \phi_{12} + \phi_{13}$$

See Figure 7 for graphs of ξ and η. Since there are exactly $(n-2)^2$ different macroelements with size $3h \times 3h$ in $\mathscr{T}_h$—the set of all these macroelements is named by $\mathscr{U}_h$—we find a basis for $\mathbf{Z}_h$. By the results of Section 4, we have

Theorem 5.1
Let $\mathscr{T}_h$ be the crisscross mesh of the unit square with $h = 1/n$. Then

$$\{\mathbf{z}^U | \forall U \in \mathscr{U}_h\}$$

DOI: 10.1002/fld

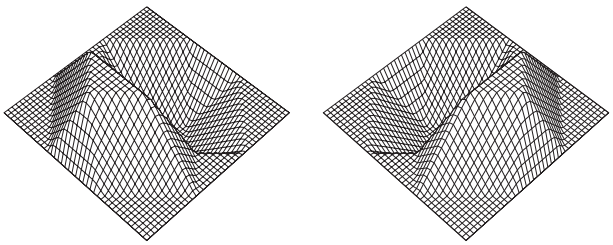

Figure 7. The shape of the two components of $\mathbf{z}^U$.

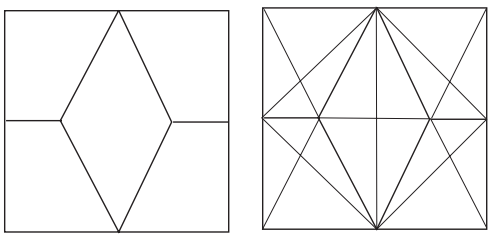

Figure 8. One macro-quadrilateral element and its crisscross-refinement.

form a basis of $\mathbf{Z}_h$. Furthermore, if $\mathbf{u} \in \mathring{\mathbf{H}}^2(\Omega)$ and $\operatorname{div} \mathbf{u} = 0$, then

$$\inf_{\mathbf{v} \in \mathbf{Z}_h} \|\mathbf{u} - \mathbf{v}\|_{1,\Omega} \leqslant Ch \|\mathbf{u}\|_{2,\Omega}$$

6. NUMERICAL TESTS

In this section, we report some results of numerical experiments. First, we calculate the reduced inf–sup constant of the element $\mathscr{P}_1$–$\mathscr{P}_0$ on a reduced-stable family, which is a crisscross-refinement of a stable quadrilateral family for the $\mathscr{Q}_1$–$\mathscr{P}_0$ element, see [25]. We consider problem (1) when Ω is the unit square. The unit square is first partitioned into $n \times n$ small squares, $2h = 1/n$. The partition is denoted by $\mathscr{Q}_{2h}$. The $\mathscr{Q}_h$ is then defined by partitioning each square of $\mathscr{Q}_{2h}$ into five quadrilaterals (see Figure 8). Finally, the triangulation $\mathscr{T}_h$ is the crisscross-refinement of $\mathscr{Q}_h$ as depicted in Figure 8.

By the work of Stenberg [25], we know the $\mathscr{Q}_1$–$\mathscr{P}_0$ element is stable on $\mathscr{Q}_h$. Therefore, $\mathscr{P}_1$–$\mathscr{P}_0$ is reduced-stable on $\mathscr{T}_h$, and $\dim N_h = 5n^2 + 1$ (Lemma 2.2). Although there is a relatively large space of spurious pressure modes involved, all these modes can be filter out from the numerical approximation p_h quite easily, quadrilateral by quadrilateral. Of course, the velocity approximation $\mathbf{u}_h$ is of the optimal order, and no recovery is needed.

The reduced inf–sup constant $\gamma_h(\mathbf{V}_h, N_h)$ and $\dim N_h$ for $1/h = 2n = 2, 4, 6, \ldots, 16$ are reported in Table I. The reduced inf–sup constant is clearly bounded below, and the bound is a relatively large number.

DOI: 10.1002/fld

Table I. Inf–sup constants for $\mathscr{P}_1$–$\mathscr{P}_0$.

h	$\gamma_h(\mathbf{V}_h, M_h)$	$\dim N_h$
1/2	0.31808	6
1/4	0.31314	21
1/6	0.31378	46
1/8	0.31481	81
1/10	0.31615	126
1/13	0.31653	181
1/14	0.31660	246
1/16	0.31693	321

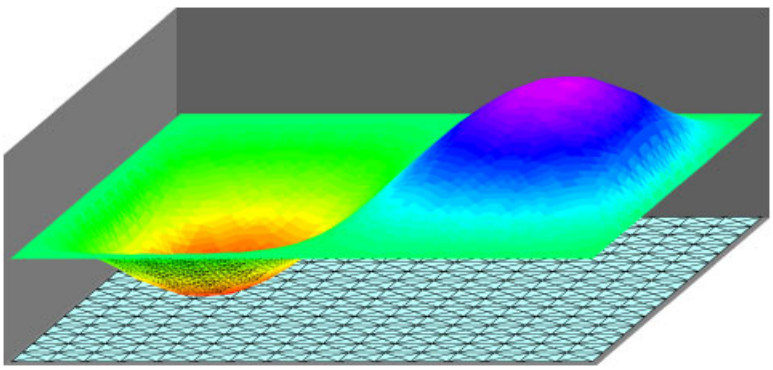

Figure 9. The first component of $\mathbf{u}_h$ on level 4 grid.

Finally, we use the newly discovered divergence-free $\mathscr{P}_1$ elements on the crisscross grids (cf. Figure 6) to solve the following model Stokes equations:

$$a(\mathbf{u}, \mathbf{v}) - b(\mathbf{v}, p) = (\mathbf{f}, \mathbf{v}) \quad \forall \mathbf{v} \in \mathbf{V}$$

$$b(\mathbf{u}_h, q) = 0 \quad \forall q \in P$$

defined on the unit square $\Omega = [0, 1]^2$, where

$$f = -\Delta \operatorname{curl} g + \nabla g_{xx} = \begin{pmatrix} -g_{yxx} - g_{yyy} - g_{xxx} \\ g_{xxx} + g_{xyy} - g_{yxx} \end{pmatrix} \tag{15}$$

with $g = 64(x - x^2)^2(y - y^2)^2$. The exact solution is

$$\mathbf{u} = \operatorname{curl} g$$

We depict the first component of $\mathbf{u}$ ($\mathbf{u}_h$ in fact) in Figure 9.

Thanks to the newly discovered divergence-free basis, problem (15) is reduced to, find $\mathbf{u}_h \in \mathbf{Z}_h$ such that

$$a(\mathbf{u}_h, \mathbf{v}) = (\mathbf{f}, \mathbf{v}) \quad \forall \mathbf{v} \in \mathbf{Z}_h \tag{16}$$

DOI: 10.1002/fld

Table II. Convergence of divergence-free $\mathscr{P}_1$ finite elements.

Level	h	# elements	$\dim \mathbf{V}_h + \dim P_h$	$\dim \mathbf{Z}_h$	$\|\mathbf{u} - \mathbf{u}_h\|_\infty$
3	1/4	64	146	4	0.21398925
4	1/8	256	546	36	0.07262499
5	1/16	1024	2114	196	0.02063174
6	1/32	4096	8322	900	0.00549276

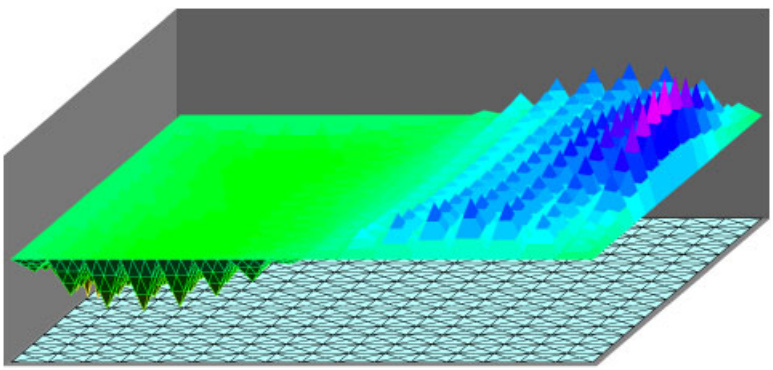

Figure 10. The first component of the error $\mathbf{u} - \mathbf{u}_h$.

where $\mathbf{Z}_h$ is the divergence-free $\mathscr{P}_1$ finite element space defined in Section 5. We note that, comparing to the traditional non-positive definite finite element systems, we have a positive definite matrix for the discrete linear system (16). Further, the number of unknowns in the finite element equations (16) is much less than one-eighth of that in the standard mixed finite element equations, see the fourth and the fifth columns of Table II. From the fifth column of Table II, it is apparent that the divergence-free finite element solution converges at the optimal order, $O(h^2)$. At the end, in Figure 10, we plot one component of error $(\mathbf{u} - \mathbf{u}_h)$ on the grid level 4. We can see that the nodal error is much larger at the crisscross points (the centre of each square), compared with that at the square vertices.

The auxiliary variable, pressure p_h, may not be wanted as it is introduced as a Lagrange multiplier. If we do want to further compute p_h after obtaining $\mathbf{u}_h$, it seems not so obvious. In the $\mathscr{P}_1$–$\mathscr{P}_0$ finite element pair $\mathbf{V}_h - M_h$, the reduced pressure space M_h is precisely the divergence of $\mathbf{V}_h$. One method might be, after $\mathbf{u}_h \in \mathbf{Z}_h$ is found, solving a $(\operatorname{div} \mathbf{w}_h, \operatorname{div} \mathbf{v}_h)$ equation by an iterative method such as the conjugate gradient method, where $\operatorname{div} \mathbf{w}_h = p_h$. However, it is painful and computational costing to project $\mathbf{w}_h$ into the orthogonal space of the divergence-free subspace $\mathbf{Z}_h$ at each step of iteration. So we use a classic method, the iterative penalty method [37], for solving the discrete Stokes equations to obtain $\mathbf{u}_h$ and p_h simultaneously as follows.

Let $u^0 = 0$ and define the iteration for $n = 1, 2, \ldots$ by

$$a(\mathbf{u}_h^n, \mathbf{v}) + r(\operatorname{div} \mathbf{u}^n, \operatorname{div} \mathbf{v}) = (\mathbf{f}, \mathbf{v}) + \left(\operatorname{div} \sum_{i=0}^{n-1} r \mathbf{u}_h^i, \operatorname{div} \mathbf{v} \right)$$

DOI: 10.1002/fld

Table III. Iterative penalty method for $\mathscr{P}_1$–$\mathscr{P}_0$ finite elements.

Level	IPM # +1	$\|\mathbf{u}-\mathbf{u}_h\|_\infty$	$\|p-p_h\|_\infty$
3	6	0.2140078967	2.7175115700
4	5	0.0726272472	1.7420730033
5	5	0.0206304055	0.9671728827
6	5	0.0054924298	0.4985045418
7	4	0.0014173141	0.2535286586

When reaching the size of truncation error (or the computer accuracy), i.e.

$$(\operatorname{div}\mathbf{u}_h^N, \operatorname{div}\mathbf{u}^N) \leqslant Ch^2 \simeq \|\mathbf{u}-\mathbf{u}_h\|_{H^1}^2$$

the iteration stops. At the end, we simply compute

$$p_h = \operatorname{div} \sum_{i=0}^{N-1} r\mathbf{u}_h^i$$

The numbers of iterative penalty iterations and the results are reported in Table III, where the data match those obtained by using the divergence-free basis.

ACKNOWLEDGEMENTS

The first author would like to thank Professor Douglas N. Arnold for his encouragement, advice, and support during the years of the author's study at the Pennsylvania State University.

REFERENCES

1. Arnold DN, Qin J. Quadratic velocity/linear pressure Stokes elements. In *Advances in Computer Methods for Partial Differential Equations*, Vichnevetsky R, Steplemen RS (eds), vol. VII, 1992.
2. Baker G, Jureidini W, Karakashian A. Piecewise solenoidal vector fields and the Stokes problem. *SIAM Journal on Numerical Analysis* 1990; **27**:1466–1485.
3. Brenner S. A nonconforming multigrid method for the stationary Stokes equations. *Mathematics of Computation* 1990; **55**:411–437.
4. Brezzi F, Fortin M. *Mixed and Hybrid Finite Element Methods*. Springer: Berlin, 1991.
5. Raviart PA, Girault V. *Finite Element Methods for Navier–Stokes Equations*. Springer: Berlin, 1986.
6. Fortin A, Fortin M. Newer and newer elements for incompressible flow. In *Finite Elements in Fluids*, Gallagher RH, Carey GF, Oden JT, Zienkie OC (eds), vol. 6, 1981; 29–48.
7. Qin J. On the convergence of some low order mixed finite elements for incompressible fluids. *Thesis*, Pennsylvania State University, 1994.
8. Scott LR, Vogelius M. Norm estimates for a maximal right inverse of the divergence operator in spaces of piecewise polynomials. *Mathematical Modelling Numerical Analysis* 1985; **9**:11–43.
9. Zhang S. A new family of stable mixed finite elements for 3D Stokes equations. *Mathematics of Computation* 2005; **74**(250):543–554.
10. Fix GJ, Gunzburger MD, Nicolaides RA. On mixed finite element methods for first-order elliptic systems. *Numerische Mathematik* 1981; **37**:29–48.
11. Powell MJD. Piecewise quadratic surface fitting for contour plotting. In *Software for Numerical Mathematics*, Evans DJ (ed.). Academic Press: New York, 1976; 253–2271.
12. Scott LR, Vogelius M. Conforming finite element methods for incompressible and nearly incompressible continua. *Lectures in Applied Mathematics* 1985; **22**:221–244.

DOI: 10.1002/fld

13. Babuška I. The finite element method with Lagrangian multipliers. *Numerische Mathematik* 1973; **20**:179–192.
14. Brezzi F. On the existence, uniqueness, and approximation of saddle point problems arising from Lagrangian multipliers. *RAIRO: Analyse Numerique* 1974; **8**:129–151.
15. Boland JM, Nicolaides RA. Stability of finite elements under divergence constraints. *SIAM Journal on Numerical Analysis* 1983; **20**:722–731.
16. Boland JM, Nicolaides RA. Stable and semistable low order finite elements for viscous flows. *SIAM Journal on Numerical Analysis* 1985; **22**:474–492.
17. Griffiths D, Silvester D. Unstable modes of the $\mathscr{Q}_1$–$\mathscr{P}_0$ element. *Numerical Analysis Report No. 257*, Department of Mathematics, University of Manchester, 1994.
18. Johnson C, Pitkäranta J. Analysis of some mixed finite element methods related to reduced integration. *Mathematics of Computation* 1982; **158**:375–400.
19. Malkus DS. Eigenproblems associated with the discrete LBB-condition for incompressible finite elements. *International Journal of Engineering Science* 1981; **19**:1299–1310.
20. Mansfield L. On finite element subspaces on quadrilateral and hexahedral meshes for incompressible viscous flow problems. *Numerische Mathematik* 1984; **45**:165–172.
21. Oden JT, Jacquotte O. Stability of some mixed finite element methods for Stokesian flows. *Computer Methods in Applied Mechanics and Engineering* 1984; **43**:231–247.
22. Pitkäranta J, Stenberg R. Analysis of some mixed finite element methods for plane elasticity equations. *Mathematics of Computation* 1983; **41**:399–423.
23. Pitkäranta J, Stenberg R. Error bounds for the approximation of the Stokes problem using bilinear/constant elements on irregular quadrilateral meshes. In *The Mathematics of Finite Elements and Applications*, Whiteman J (ed.), vol. V. Academic Press: London, 1985; 325–334.
24. Sani RL, Gresho PM, Lee RL, Griffiths D. The cause and cure(?) of the spurious pressures generated by certain FEM solutions of the incompressible Navier–Stokes equations. *International Journal for Numerical Methods in Fluids* 1981; **1**:171–204.
25. Stenberg R. Analysis of mixed finite element methods for the Stokes problem: a unified approach. *Mathematics of Computation* 1984; **42**:9–23.
26. Bernstain B, Feigl KA, Olsen T. A first-order exactly incompressible finite element for axisymmetric fluid flow. *SIAM Journal on Numerical Analysis* 1996; **33–5**:1736–1758.
27. Powell MJD, Sabin MA. Piecewise quadratic approximations on triangles. *ACM Transactions on Mathematical Software* 1977; **3–4**:316–325.
28. Heindl G. Interpolation and approximation by piecewise quadratic C1-functions of two variables. *International Schriftenreihe Numerical Mathematics* 1979; **51**:146–161.
29. Lai M-J. Scattered data interpolation and approximation using bivariate C1 piecewise cubic polynomials. *Computer Aided Geometric Design* 1996; **13**:81–88.
30. Nürnberger G, Rayevskaya V, Schumaker LL, Zeilfelder F. Local Lagrange interpolation with bivariate splines of arbitrary smoothness. *Constructive Approximation* 2006; **23**:33–59.
31. Liu H, Hong D, Cao D-Q. Bivariate C^1 cubic spline space over a nonuniform type-2 triangulation and its subspaces with boundary conditions. *Computers and Mathematics with Applications* 2005; **49**:1853–1865.
32. Nürnberger G, Zeilfelder F. Developments in bivariate spline interpolation. *Journal of Computational and Applied Mathematics* 2000; **121**:125–152.
33. Sorokina T, Zeilfelder F. Optimal quasi-interpolation by quadratic C^1-splines on type-2 triangulations. *Approximation Theory XI*, Gatlinburg, 2004. Mod. Methods Math. Nashboro Press: Brentwood, TN, 2005; 423–438.
34. Nürnberger G, Rössl C, Seidel H-P, Zeilfelder F. Quasi-interpolation by quadratic piecewise polynomials in three variables. *Computer Aided Geometric Design* 2005; **22**:221–249.
35. Schumaker LL, Sorokina T. A trivariate box macroelement. *Constructive Approximation* 2005; **21**(3):413–431.
36. Hangelbroek T, Nürnberger G, Rössl C, Seidel H-P, Zeilfelder F. Dimension of C^1-splines on type-6 tetrahedral partitions. *Journal of Approximation Theory* 2004; **131**:157–184.
37. Brenner SC, Scott LR. *The Mathematical Theory of Finite Element Methods*. Springer: New York, 1994.

DOI: 10.1002/fld